Protein Design of a Bacterially Expressed HIV-1 gp41 Fusion Inhibitor†

Yiqun Deng,‡ Qi Zheng,‡ Thomas J. Ketas,§ John P. Moore,§ and Min Lu*,‡

Department of Biochemistry and Department of Microbiology and Immunology, Weill Medical College of Cornell University, New York, New York 10021

Received January 22, 2007; Revised Manuscript Received February 13, 2007

ABSTRACT: Peptides derived from the carboxyl-terminal heptad repeat of the gp41 envelope glycoprotein ectodomain (C-peptides) can inhibit HIV-1 membrane fusion by binding to the amino-terminal trimeric coiled coil of the same protein. The fusion inhibitory peptide T-20 contains an additional tryptophan-rich sequence motif whose binding site extends beyond the gp41 coiled-coil region yet provides the key determinant of inhibitory activity in T-20. Here we report the design of a recombinant peptide inhibitor (called C52L) that includes both the C-peptide and tryptophan-rich regions. By calorimetry, C52L binds to a peptide mimic of the amino-terminal coiled coil with a K_d of 80 nM, reflecting the large degree of helicity in C52L as measured by circular dichroism spectroscopy. The C52L peptide potently inhibits *in vitro* infection of human T cells by diverse primary HIV-1 isolates irrespective of coreceptor preference, with nanomolar IC_{50} values. Significantly, C52L is fully active against T-20-resistant variants in a single-cycle HIV-1 infectivity assay. Moreover, because it can be expressed in bacteria, the C52L peptide might be more economical to manufacture on a large scale than T-20-like peptides produced by chemical synthesis. Hence the C52L fusion inhibitor may find a practical application, for example as a vaginal or rectal microbicide to prevent HIV-1 infection in the developing world.

The use of combination therapy including protease and reverse transcriptase inhibitors (called highly effective antiretroviral therapy, HAART[1]) has markedly reduced the progression of human immunodeficiency virus type 1 (HIV-1) infection to AIDS and improved the health of many patients. HAART cannot, however, eradicate the virus from infected individuals, and its effectiveness is often tempered by toxic side effects, long-term adverse reactions, lack of adherence, and the emergence of drug-resistant HIV-1 variants (*1*−*6*). Hence new classes of anti-HIV-1 drugs directed at targets other than viral protease or reverse transcriptase are urgently needed, to curb the global epidemic of HIV-1 infection. One such antiviral drug is the fusion inhibitor enfuvirtide (T-20), which is used as salvage therapy for a growing number of AIDS patients who no longer respond to HAART (*7*). However, the clinical use of T-20 is limited by resistance development, the requirement for parenteral delivery, and the high cost of chemical synthesis. Despite intensive efforts, the search for orally bioavailable, small-molecule HIV-1 fusion inhibitors targeting gp41 has been frustrating. Moreover, inhibitors of virus-cell fusion are under consideration as topical microbicides to prevent HIV-1 sexual transmission (*8*, *9*). New peptidic fusion inhibitors with greater potency and an improved spectrum of activity would be useful for therapeutic and microbicidal applications.

Entry of HIV-1 into its target cell to establish an infection requires fusion of the viral and cellular membranes, a process mediated by the viral envelope glycoprotein (Env) and receptors on the host cell surface. HIV-1 Env is synthesized as the polyprotein precursor gp160 that oligomerizes in the endoplasmic reticulum and is subsequently cleaved by a cellular protease to yield the receptor-binding (gp120) and membrane fusion (gp41) subunits (*10*). The mature Env complex is a trimer, with three gp120 glycoproteins associated noncovalently with three membrane-anchored gp41 subunits. Binding of gp120/gp41 to cellular receptors (CD4 and a coreceptor, such as CXCR4 or CCR5) triggers a series of conformational changes in gp41 that ultimately leads to formation of a postfusion trimer-of-hairpins structure and thereby effects membrane fusion (*11*−*13*). The ectodomain of gp41 includes two conserved regions consisting of heptad repeats (HR) of hydrophobic residues characteristic of coiled coils. The first (HR_N) is adjacent to the N terminus of gp41 while the second (HR_C) immediately precedes the transmembrane domain (Figure 1a). Peptides derived from these regions are referred to as N-peptides and C-peptides, respectively. The soluble core of the gp41 trimer-of-hairpins is a bundle of six α-helices: a central trimeric coiled coil formed by the N-peptide region is surrounded by three C-peptide helices that bind to conserved hydrophobic grooves on the coiled-coil surface in an antiparallel orientation (*14*−*17*) (Figure 1b). During the fusion process, the fusion peptide at the extreme N terminus of gp41 is exposed and

† This work was supported by NIH Grants U19 AI65413 and R01 AI68591 and by the Irma T. Hirschl Trust. The Department of Microbiology and Immunology at the Weill Medical College gratefully acknowledges the support of the William Randolph Hearst Foundation.

* To whom correspondence should be addressed. Phone: (212) 746-6562. Fax: (212) 746-8875. E-mail: mlu@med.cornell.edu.

‡ Department of Biochemistry.

§ Department of Microbiology and Immunology.

[1] Abbreviations: HAART, highly effective anti-retroviral therapy; HIV-1, human immunodeficiency virus type 1; Env, envelope glycoprotein; HR, heptad repeat; HPLC, high-performance liquid chromatography; CNBr, cyanogen bromide; CD, circular dichroism; TBS, Tris-buffered saline; GuHCl, guanidine hydrochloride; $[\theta]_{222}$, molar ellipticity at 222 nm; PBMCs, human peripheral blood mononuclear cells; RLU, relative light units.

10.1021/bi7001289 CCC: $37.00
Published on Web 03/20/2007

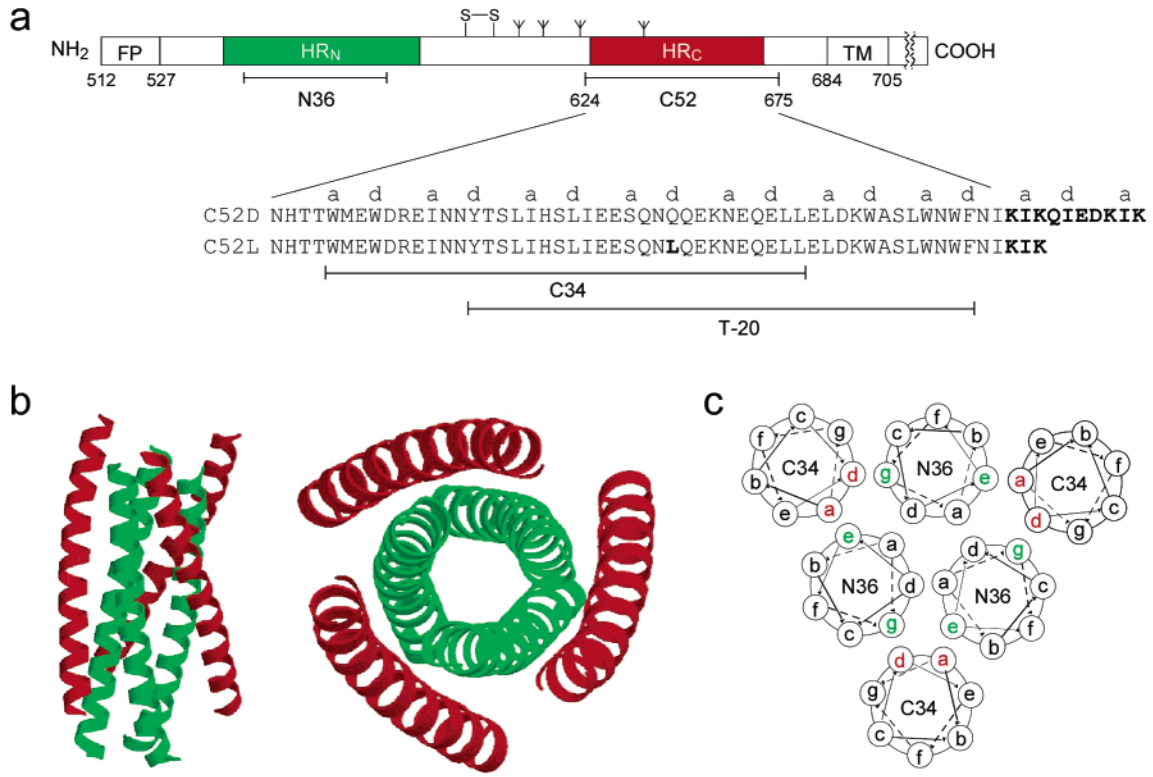

FIGURE 1: HIV-1 gp41 structure and fusion inhibitors. (a) Schematic diagram of gp41. The positions of the fusion peptide (FP), the two hydrophobic heptad repeats (HR_N and HR_C), the disulfide bond (S−S), the potential *N*-linked glycosylation sites, and the transmembrane region (TM) are shown. The locations of T-20 (enfuvirtide), N36 (N-peptide), and C34 (C-peptide) are indicated. The sequence of the C52 segment is shown, along with the heptad *a* and *d* positions. The engineered C52D and C52L peptides used in this study contain the C-terminal Lys-Ile-Lys-Gln-Ile-Glu-Asp-Lys-Ile-Lys and Lys-Ile-Lys sequences, respectively (see text). The Gln652 to leucine substitution in C52L is shown in bold. Residues are numbered according to their position in the HIV-1_{HXB2} gp160 sequence. (b) Lateral (left) and axial (right) views of a six-helix bundle formed by the N36 and C34 peptides (PDB 1AIK). The N termini of the N36 helices point toward the top of the page, and those of the C34 helices point toward the bottom. (c) Helical wheel representations of N36 and C34. Heptad-repeat positions are labeled *a* through *g*. The *a* and *d* residues in the C-peptide (red) interact with the exposed *e* and *g* side chains on the central N-peptide coiled coil (green).

inserted into the target cell membrane (*18*). Thus a folding-back of the gp41 ectodomain drives the C-terminal transmembrane anchor toward the fusion peptide to bring the viral and cellular membranes into proximity, thereby facilitating membrane fusion and subsequent viral entry (*14*−*16*).

The HIV-1 entry process is a primary target for vaccine and drug development. Synthetic C-peptides, such as C34 and T-20 (see Figure 1a), are potent inhibitors of HIV-1 infection and syncytium formation (*19*−*21*). The available evidence indicates that these C-peptide mimics interfere with formation of the gp41 six-helix bundle in a dominant-negative manner by binding to the transiently exposed N-peptide coiled coil in a "prehairpin" intermediate (*17*, *22*−*25*). C-peptides exist in a random-coil configuration in isolation and form an α-helical structure only when bound to their target, the N-peptide region of gp41 (*14*−*17*, *20*, *26*). Hence the presentation of C-peptides in a preformed α-helical conformation may be a viable strategy to improve their inhibitory potency (*27*−*31*). The crystal structure of the gp41 core reveals that residues at positions *a* and *d* of the C-peptide helix pack against the *e* and *g* side chains on the surface of the N-peptide coiled-coil trimer (*14*−*16*). Consistent with this model, replacement of a buried polar residue (Gln652) at a *d* position of C-helix by the nonpolar leucine side chain imparts additional binding energy and results in a ~3-fold increase in antiviral activity of the mutant C-peptide (*28*). In the present study, we have applied a protein-engineering approach to develop recombinant peptides in which short coiled-coil segments are fused to the C terminus of the gp41 C-peptide. These chimeric molecules, which present the C-peptide in an α-helical conformation, inhibit the replication of diverse HIV-1 isolates including T-20-resistant strains *in vitro* at nanomolar concentrations. The engineered C-peptides can be expressed in bacteria and produced economically. The potent and inexpensive gp41 fusion inhibitors described here may have potential utility as a therapeutic drug, and also as a microbicide for preventing HIV-1 sexual transmission in developing countries.

MATERIALS AND METHODS

Plasmid Construction and Protein Production. Recombinant DNA procedures were carried out by standard methods; all generated sequences were confirmed by DNA sequencing. Plasmid pC52D encoding C52D was constructed by subcloning the C52 segment (representing residues 624−675 of HIV-1 HXB2 gp160) followed by a Lys-Ile-Lys-Gln-Ile-Glu-Asp-Lys-Ile-Lys sequence (see Figure 1a) into the pAED4 vector (*32*). Plasmid pC52L encoding C52L was prepared using pC52D as the template. Mutations were introduced using the method of Kunkel (*33*). The C52D and C52L peptides were expressed in *Escherichia coli* BL21-(DE3)/pLysS (Novagen). The cells were grown at 37 °C in LB medium to an optical density of 0.7 at 600 nm and harvested by centrifugation 4 h postinduction with 0.5 mM

IPTG. Bacterial pellets were resuspended in buffer A (50 mM Tris-HCl, 1 mM EDTA, pH 8.0) supplemented with 25% sucrose. The cells were lysed by sonication and centrifuged (35000*g* for 15 min) to separate the soluble fraction from inclusion bodies. The inclusion bodies were washed extensively with buffer A containing 1% Triton X-100. The peptide was purified directly from the inclusion bodies after resuspension in 8 M urea/buffer A. The debris was removed by a 1 h centrifugation at 4 °C. The peptide was then loaded onto a DEAE Sepharose column (Pharmacia) equilibrated with 3 M urea/buffer A and eluted using a NaCl gradient (0 to 1000 mM) in 3 M urea/buffer A. The sample was dialyzed into 5% (vol/vol) acetic acid overnight at 4 °C. The peptide was purified to homogeneity by reverse-phase HPLC (Waters) on a Vydac C18 preparative column (Hesperia, CA) using a water−acetonitrile gradient in the presence of 0.1% trifluoroacetic acid and lyophilized.

The C52 construct with the Met629 → Leu mutation was appended to the *TrpLE′* leader sequence (*68*). The $C52_{M629L}$ peptide was expressed as a chimeric protein in *E. coli* BL21 (DE3)/pLysS, purified from inclusion bodies, and cleaved from the *TrpLE′* leader sequence with cyanogen bromide (CNBr) as described (*57*). The T-20 and C34 peptides were synthesized by standard fluorenylmethoxycarbonyl chemistry with acetylated N terminus and amidated C terminus. After cleavage from the resin, the peptides were desalted on a Sephadex G-25 column (Pharmacia) and lyophilized. Peptides were then purified by reverse-phase HPLC as described above. The untagged 5-helix protein used for the isothermal calorimetric binding experiments was expressed in *E. coli* BL21(DE3)/pLysS with the pAED4 vector (*32*), extracted from inclusion bodies, refolded by renaturation from urea, and purified by ion exchange and size-exclusion chromatography as previously described (*34*). Protein identities were confirmed by electrospray mass spectrometry (Voyager Elite; PerSeptive Biosystems, Framingham, MA). The concentrations of all peptide proteins were determined by tryptophan and tyrosine absorbance (at 280 nm) in 6 M guanidine hydrochloride (GuHCl) (*35*). Stock solutions of 500 μM of C-peptides in 50 mM Tris-HCl (pH 8.0) were prepared, frozen in aliquots, and stored at −20 °C. Control experiments demonstrated that the inhibitory activity of these peptides was not affected by freezing.

Circular Dichroism Spectroscopy. CD experiments were performed on an Aviv 62A/DS (Aviv Associates, Lakewood, NJ) spectropolarimeter equipped with a thermoelectric temperature control at 10 μM peptide concentration in TBS (50 mM Tris-HCl, pH 8.0, 150 mM NaCl). CD spectra were collected from 260 to 200 nm at 0 °C, using an average time of 5 s, a cell path length of 0.1 cm, and a bandwidth of 1 nm. A $[\theta]_{222}$ value of $-33\,000$ deg cm^2 dmol^{-1} was taken to correspond to 100% helix (*36*). Thermal stability was determined by monitoring $[\theta]_{222}$ as a function of temperature. Thermal melts were performed in 2 deg intervals with a 2 min equilibration at the desired temperature and an integration time of 30 s.

Sedimentation Equilibrium Analysis. Analytical ultracentrifugation measurements were carried out on a Beckman XL-A analytical ultracentrifuge (Beckman Coulter, Fullerton, CA) equipped with an An-60 Ti rotor. Protein samples were dialyzed overnight into TBS (pH 8.0), loaded at initial concentrations of 10, 30, and 100 μM, and analyzed at rotor speeds of 21, 24, and 35 krpm for C52D, and 25, 28, and 35 krpm for C52L at 4 and 37 °C. Data were acquired at two wavelengths per rotor speed setting and processed simultaneously with a nonlinear least-squares fitting routine (*37*). Solvent density and protein partial specific volume were calculated according to solvent and protein composition, respectively (*38*).

Isothermal Titration Calorimetry. Isothermal titration calorimetry measurements were performed on a VP-isothermal titration calorimeter (MicroCal, Amherst, MA) thermostated at 37 °C. Peptides were dialyzed overnight into 25 mM Tris-HCl, pH 8.0, 50 mM NaCl using a 2 kDa molecular mass cutoff Spectra/Por membrane. All solutions were degassed before the experiment. C-peptides ranging from 1.0 to 1.5 mM were injected in 2 μL of increments into the reaction cell (1.42 mL volume) containing 20 μM 5-helix. The heat associated with the binding reaction was obtained by subtracting the heat of dilution of C-peptide from the heat of reaction with 5-helix. Binding isotherms were analyzed by fitting the data to a single binding site model with the Microcal (Amherst, MA) ORIGIN analysis software.

Cell-to-Cell Fusion Assay. Syncytia formation was assayed by coculturing CHO[HIVe] (clone 7d2) cells expressing HXB2 envelope and tat (*39*) with U373-MAGI cells (M. Emerman and A. Geballe, National Institutes of Health AIDS Research and Reference Reagent Program) in the presence of different concentrations of C-peptide inhibitor. Cell fusion allows the expression of nuclear β-galactosidase from the U373-MAGI indicator cell line and can be quantitated by monitoring β-galactosidase activity. After an overnight incubation at 37 °C after coculture, β-galactosidase enzymatic activity was measured with the Mammalian beta-galactosidase Chemiluminescent Assay Kit (Gal-Screen from Applied Biosystems). The peptide inhibitor concentrations at which activities were reduced by 50% (IC_{50}) and 90% (IC_{90}) relative to control samples lacking C-peptide were calculated by fitting data to the variable-slope-sigmoid equation using the Prism program (Graphpad, San Diego, CA).

Inhibition of HIV-1 Replication in PBMC Cells. Human peripheral blood mononuclear cells (PBMCs) were isolated from healthy blood donors by Ficoll-Hypaque gradient centrifugation and stimulated in three separate pools treated with phytohemagglutinin (PHA) at 5 μg/mL, PHA at 0.5 mg/mL, or anti-CD3 antibody OKT3 essentially as previously described (*40*). After 3 day stimulation, the pools were mixed immediately prior to their use in the antiviral assay (*41*). In brief, serial dilutions of C-peptide (50 μL) were incubated with 50 μL aliquots of virus inoculum (400 to 1000 $TCID_{50}$/mL) for 1 h at 37 °C. The mixtures of C-peptide inhibitor with virus were then combined with 2×10^5 PBMCs (100 μL/well). On days 5−7 postinfection, the extent of HIV-1 replication was determined by measuring the p24 antigen content of the culture supernatants by ELISA (*42*). As the virus inoculum was not washed out at any stage of the experiment, the residual input p24 concentration was subtracted from all test results. Peak virus production in the absence of C-peptide inhibitor was designated as 100%, and IC_{50} and IC_{90} values were calculated by variable-slope-sigmoid analysis using the Prism graph software. The cytotoxic effect of C-peptides on PBMCs was measured in the presence of serially diluted inhibitors for 6 days, and cell viability was quantitated by using a MTT assay (*43*).

Inhibition of HIV-1 Env-Pseudotyped Virion Infection. The generation of Env-pseudotyped virus stocks in 293T cells by calcium phosphate transfection and the use of the engineered HIV-1 coreceptor-bearing cell line U87-CD4$^+$-CCR5$^+$ (3000 cells per well) for Env-pseudotyped virus infection have been described previously (*44*−*46*). Briefly, the envelope genes were amplified by PCR, cloned into an expression vector, and cotransfected with an envelope-defective proviral plasmid to generate pseudotyped luciferase-encoding viruses. Variant envelopes were generated using QuikChange site-directed mutagenesis kit (Stratagene, La Jolla, CA) and verified by DNA sequencing. Recombinant viruses were used to infect U87-CD4$^+$-CCR5$^+$ cells (3000 cells per well) in the presence of varying concentrations of C-peptide. The amount of input pseudovirus was normalized by infectivity (virus titer) rather than by p24 antigen content. Luciferase activity in the target cells was measured in relative light units (RLU) 72 h after infection. For each C-peptide, data from duplicate measurements were fit to the variable-slope-sigmoid equation to obtain IC_{50} values.

RESULTS

Design of C52D and C52L. The 52-residue C-peptide of HIV-1 gp41 (denoted C52) includes the C34 and T-20 regions that have been shown to be essential for anti-HIV-1 activity (*17*, *19*, *20*, *26*, *47*, *48*) (Figure 1a). C34 identified by the protein-dissection method corresponds to the outer-layer C-peptide helix of the postfusion six-helix bundle (Figure 1b) (*26*). The inhibitory activity of C34 depends on its ability to bind to a prominent hydrophobic pocket in the gp41 coiled-coil N-peptide region (*14*−*16*, *48*−*51*). Interestingly, T-20 lacks pocket-binding residues yet contains a C-terminal Trp-Asn-Trp-Phe sequence (at positions 670−673) that is essential to maintain its anti-HIV-1 potency (*20*), despite the fact that this region does not directly participate in the six-helix bundle structure (*14*−*16*, *26*, *52*). Moreover, C-peptides that contain pocket-binding residues, such as C34, are fully active *in vitro* against T-20-resistant viral strains (*53*). Taken together, these observations suggest that the target for the antiviral effect of T-20 may be distinct from that of C34 (*52*, *54*, *55*). A second-generation C-peptide inhibitor, T-1249, designed to overcome viral resistance to T-20, includes the additional N-peptide pocket-binding sequence and demonstrates enhanced potency and a different resistance profile (*56*). On the basis of these structure−activity considerations, we have chosen the C52 sequence as a candidate for development of a recombinant C-peptide fusion inhibitor (Figure 1a). However, our initial efforts to express isolated C52 in *E. coli* produced low yields of peptide.

T-20 and C34 are essentially unfolded in isolation (*17*, *24*, *26*), but α-helical when bound to the gp41 N-terminal coiled coil (*14*−*17*, *24*). Because this coil−helix transition should exact a large energetic penalty due to the loss of conformational entropy, stabilizing the C-peptide helix in the unbound state is a potentially powerful strategy for increasing its anti-HIV-1 potency (*27*, *29*−*31*). In effect, C52 is also largely unstructured in solution (*17*); the lack of strong α-helical character in this molecule might explain its instability in bacterial cells. We thus sought to increase the propensity of C52 to adopt a preformed α-helical conformation. Based on our accumulated knowledge of the coiled-coil motif (*57*, *58*), we placed in heptad register either 3 or 10 residues from the N terminus of a GCN4-pII isoleucine trimer (*59*) at the C terminus of C52 (see Figure 1a). The resulting chimeric peptides were referred to as C52D and C52L, respectively. We reasoned that the short GCN4-pII segments would promote C52-helix formation yet with limited intermolecular coiled-coil assemblies, because C-peptide fusion inhibitors must be monomeric to be active (see Figure 1c) (*17*, *22*). We have also mutated the buried polar Gln652 residue to leucine in the C52L construct to strengthen its interaction with the N-peptide coiled coil by providing additional hydrophobic packing forces and removing the buried polar side chain (*28*).

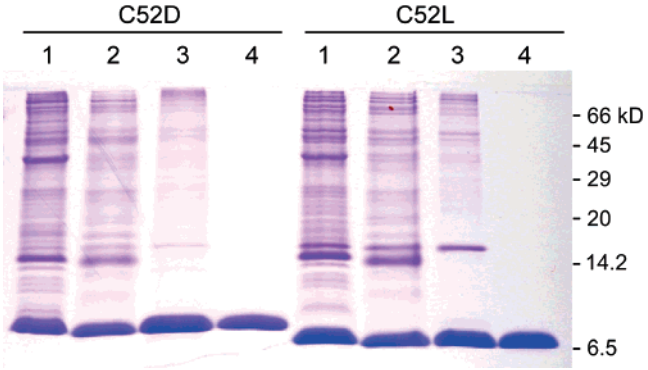

FIGURE 2: Bacterial expression and purification of the engineered C52D and C52L peptides. Samples containing 5 μg of protein were analyzed by SDS−PAGE on a 16% tricine gel with Coomassie blue staining. Lane 1, whole cell preparation; lane 2, inclusion body preparation; lane 3, DEAE Sepharose column-purified peptide; lane 4, reverse-phase HPLC-purified peptide. The sizes of protein molecular weight markers are indicated at the right.

Protein Expression and Purification. The C52D and C52L constructs were cloned into a modified pET3a vector (Novagen) using standard molecular biology techniques. The C52D and C52L peptides were prepared by expression in *E. coli* followed by extraction from insoluble bacterial inclusion bodies (see Materials and Methods). The peptides were purified by ion-exchange chromatography directly from the inclusion bodies solubilized in urea (Figure 2). Final purification by reverse-phase HPLC gives a homogeneous preparation. The N-terminal sequence analysis of the purified peptides revealed the desired sequence over five cycles of Edman degradation, with the initial Met residue retained; electrospray mass spectrometry confirmed their expected composition. In simple shake flask growth experiments, protein expression levels were up to ∼145 mg and 85 mg of peptide per liter of culture for C52D and C52L, respectively.

Helical Content and Oligomerizatoin State. The far UV circular dichroism (CD) spectra of the engineered C52D and C52L peptides are typical of an α-helix, with the characteristic minima at 208 and 222 nm in TBS (pH 8.0) at 0 °C and 10 μM peptide concentration (Figure 3a). The mean residue ellipticities at 222 nm ($[\theta]_{222}$, a measure of helical content) of C52D and C52L under these conditions are −22 000 and −16 000 deg cm^2 dmol^{-1}, consistent with ∼70 and 50% helical structure, respectively. These values are concentration-dependent, reflecting formation of the intermolecular peptide complexes at low temperatures (see below). In contrast, the spectrum of the "wild-type" $C52_{M294L}$ peptide exhibits a much weaker minimum at 222 nm and a

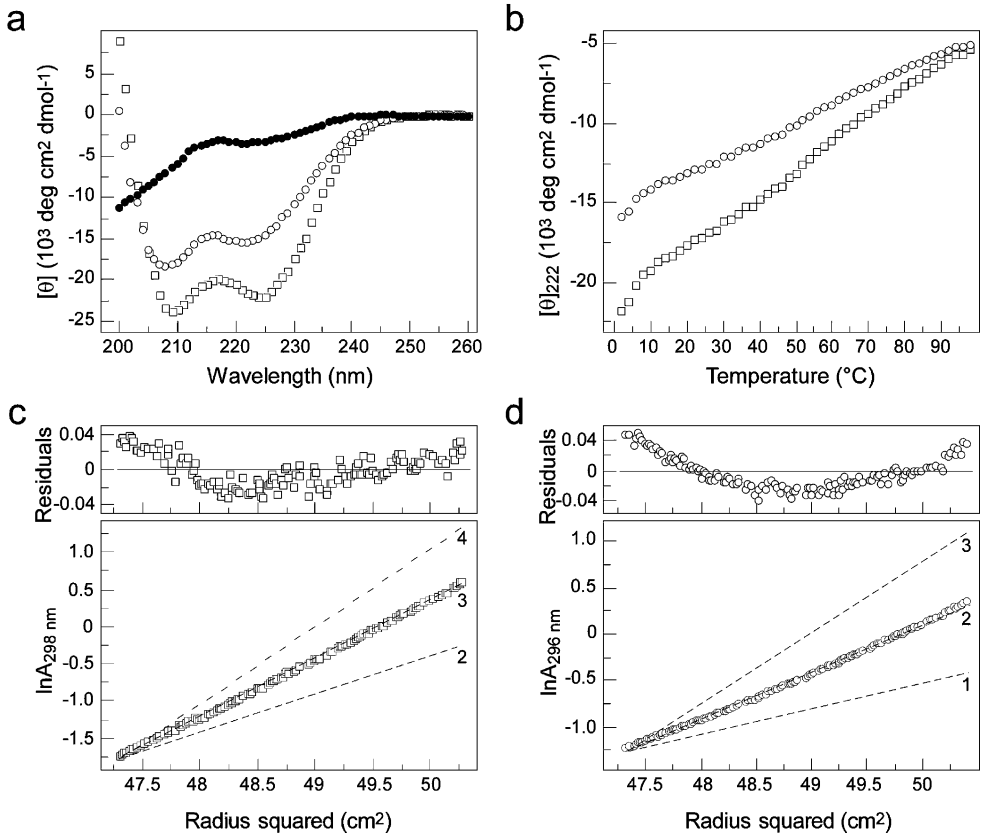

FIGURE 3: Biophysical properties of C52D and C52L. (a) Circular dichroism spectra of C52D (open squares), C52L (open circles), and $C52_{M629L}$ (filled circles) at 0 °C in TBS (pH 8.0) at a peptide concentration of 10 μM. (b) Thermal melts monitored by the circular dichroism signal at 222 nm. (c) Equilibrium ultracentrifugation data (24 krpm) for C52D (100 μM) collected in TBS (pH 8.0) at 4 °C. Dashed lines with increasing slopes indicate, respectively, the predicted data for dimer, trimer, and tetramer bundles. The deviation in the data from the linear fit for a trimeric model is plotted (upper). (d) Equilibrium ultracentrifugation data (25 krpm) for C52L (100 μM) collected in TBS (pH 8.0) at 4 °C. The deviation in the data from the linear fit for a dimeric model is plotted (upper).

more intense minimum around 200 nm, indicative of being largely in the unfolded state (Figure 3a). Both C52D and C52L lack a "folded" baseline at low temperatures and display a broad noncooperative thermal unfolding transition (Figure 3b), indicating a noncooperative disruption of the helical structure with increasing temperature. Analytical ultracentrifugation experiments at 4 °C indicate that C52D sediments as a trimeric species with no systematic dependence of apparent molecular mass on protein concentration from 10 to 100 μM (Figure 3c), while C52L is dimeric over this 10-fold concentration range (Figure 3d). However, analysis of residual differences from the trimeric and dimeric models reveals a systematic error, suggesting that both the peptides are prone to aggregation. The monomeric forms of C52D and C52L at 37 °C were demonstrated by analytical ultracentrifugation (data not shown). These results indicate that C52D and C52L associate intermolecularly to form a partially folded α-helical structure under native conditions (low temperature). Thus the added coiled-coil sequences appear to stabilize the α-helical conformation of the parent C52 peptide and clearly play an important role in determining interhelical interaction specificity at low temperatures. This helix-stabilizing effect may underlie the high-level expression of the recombinant C52D and C52L constructs in *E. coli*.

Binding Affinity to the N-peptide Coiled-Coil Trimer. It has been found that the binding affinity of C-peptides to the gp41 N-peptide region tends to correlate with their inhibitory potency (*28*, *48*). A designed 5-helix protein containing a single high-affinity binding site for C-helix inhibits HIV-1 membrane fusion by preventing six-helix bundle formation (*60*). We therefore performed isothermal titration calorimetry on the binding of C52D and C52L to 5-helix at 37 °C to investigate whether a large degree of helicity in these engineered peptides as measured by CD spectroscopy can impart favorable binding to the triple-stranded N-peptide coiled coil. Like the C34 peptide, C52D and C52L interact with the 5-helix protein in a 1:1 molar ratio; all titrations are consistent with a two-state transition, although there is a slight baseline artifact in the case of C52D (Figure 4; Table 1). C52D and C52L exhibit strong binding to 5-helix with dissociation constant (K_d) values of 25 and 80 nM, respectively. Under the same experimental conditions, C34 shows >1 order of magnitude weaker binding, with a K_d of 0.82 μM. The thermodynamic basis of the high binding affinity of C52D and C52L compared with C34 is due to a larger gain of binding entropy with a concomitant loss of binding enthalpy (see Table 1). Overall, this enthalpy−entropy compensation results in a higher binding affinity.

Inhibition of Cell−Cell Fusion by C52D and C52L. We determined the inhibitory activity of the engineered C52D and C52L peptides by cocultivating effector CHO cells (stably expressing HIV-1 Env) with target U373-MAGI cells (stably expressing CD4 and CXCR4) in the presence of varying peptide concentrations (Figure 5). C52D and C52L are potent inhibitors of cell−cell fusion (i.e., syncytia formation), with IC_{50} values of 11.7 and 1.2 nM, respectively. For comparison, the IC_{50} values of C34 and T-20 are 1.9

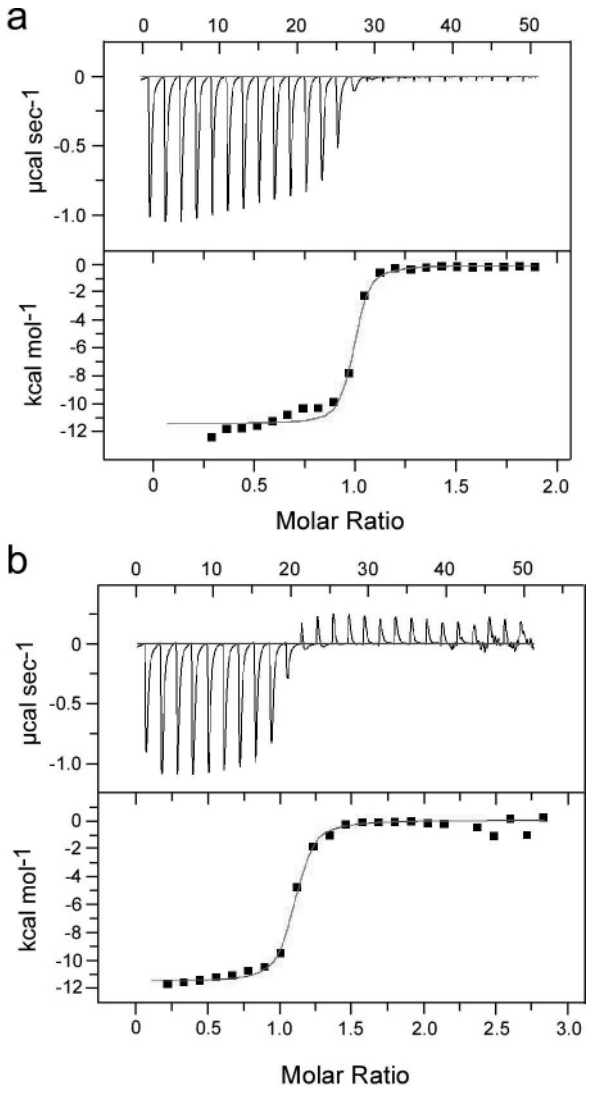

FIGURE 4: Isothermal titration calorimetry of 5-helix with C52D and C52L. Isothermal calorimetric titration measurements were carried out in TBS (pH 8.0) at 37 °C. The binding isotherms for formation of the 5-helix/C-peptide complex were graphed and normalized to the concentration of the injected peptide. (a) Titration of 5-helix with C52D. (b) Titration of 5-helix with C52L. The thermodynamic parameters after fitting to a single binding-site model are listed in Table 1.

and 18.4 nM, respectively. These results demonstrate that C52D and C52L can be used as the basis for the development of HIV-1 fusion inhibitors with structured helical conformations and improved pharmacological properties. Since C52L is approximately 10-fold more potent than C52D, the entropic gain in binding energy from the preformed α-helical structure of C52D (see above) is likely offset by the energy required to attain the active conformation of the bound state. Thus a key issue in future protein engineering efforts is to balance the changes in binding enthalpy and entropy.

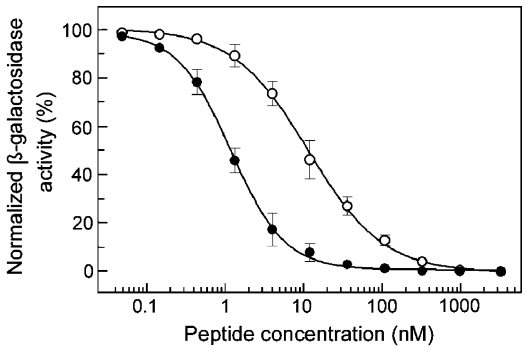

FIGURE 5: Peptide inhibition of HIV-1 Env-mediated cell−cell fusion. The C52D (open circles) and C52L (filled circles) peptides were tested for their ability to inhibit fusion between CHO gp160 (effector) and U373-MAGI (target) cells. β-Galactosidase activity measured in the target cells was normalized to 100% relative to that observed in the absence of peptide. The data represent the mean and standard error of three independent experiments, each performed in duplicate.

Peptide Inhibition of HIV-1 Infection. We evaluated the effect of the C52D and C52L peptides on HIV-1 infectivity using a diverse set of primary isolate strains with different geographic origins and coreceptor requirements (Table 2). C52D and C52L potently block the spreading infection of all of the tested clade A−F viruses in PBMC culture (as measured by the amount of p24 antigen in cell-free medium), with median IC_{50} values of 33 nM (range 10−300 nM) and 15 nM (5−61 nM), respectively. For comparison, C34 and T-20 show median IC_{50} values of 12 nM (range 4−53 nM) and 59 nM (17−149 nM), respectively. All of these peptides at 1 μM show no cytotoxicity in PBMCs as determined by a MTT assay (data not shown). It may be notable that C52L displays slightly (∼2-fold) higher antiviral activity than C52D in the viral infectivity assay but is close to an order of magnitude more potent in the cell−cell fusion assay (see Figure 5). It is possible that the stable, helical structure of C52D as determined by CD spectroscopy (Figure 4a and b) gives rise to an increased resistance to proteolytic degradation compared with C52L over the course of the 6 day infectivity experiment, thereby contributing to the potent inhibitory activity. We conclude that the recombinant C52D and C52L peptides display a broad profile of antiviral activity across HIV-1 group M viruses regardless of the particular chemokine receptor used for viral entry. A more comprehensive study of the cross-subtype activity of C52L against 25 primary CCR5-using, 12 CXCR4-using, and 7 dual-tropic isolates from subtypes A−G confirms this finding (*61*).

Inhibition of T-20-Resistant HIV-1 Variants by C52L. The use of T-20 in patients resulted in the inevitable emergence of drug-resistant HIV-1 variants (*62*−*65*). Escape-virus variants are also readily derived upon continuous *in vitro* passaging of HIV-1 in the presence of increasing T-20 concentrations (*53*). Sequence analysis of both the resistant

Table 1: Thermodynamic Parameters for C-Peptide Binding the 5-Helix Protein[a]

	N	K_d (nM)	ΔH (kcal mol^{-1})	$-T\Delta S$ (kcal mol^{-1})	ΔG (kcal mol^{-1})
C52D	0.97 ± 0.01	25.8 ± 7.1	−11.3 ± 0.5	0.5 ± 0.4	−10.8 ± 0.2
C52L	1.06 ± 0.01	80.6 ± 5.4	−11.7 ± 0.2	1.6 ± 0.3	−10.1 ± 0.1
C34	1.05 ± 0.01	809 ± 90.7	−24.4 ± 1.2	15.8 ± 1.3	−8.6 ± 0.3

[a] Values are mean and standard error of two measurements.

Table 2: HIV-1 Inhibitory Activity of the C52D and C52L Peptides[a]

			C52D ($n = 6$)		C52L ($n = 6$)		T-20 ($n = 12$)		C34 ($n = 12$)	
isolate	clade	coreceptor	IC_{50} (nM)	IC_{90} (nM)	IC_{50} (nM)	IC_{90} (nM)	IC_{50} (nM)	IC_{90} (nM)	IC_{50} (nM)	IC_{90} (nM)
DJ258	A	CCR5	26 ± 27	81 ± 87	16 ± 18	45 ± 40	25 ± 20	86 ± 74	11 ± 11	34 ± 33
JFRL	B	CCR5	16 ± 23	62 ± 86	13 ± 11	50 ± 49	18 ± 27	75 ± 81	16 ± 12	64 ± 73
NL4-3	B	CXCR4	52 ± 36	91 ± 65	25 ± 5	63 ± 27	50 ± 39	117 ± 128	13 ± 5	27 ± 6
case C 7/86	B	CXCR4/CCR5	66 ± 65	118 ± 117	38 ± 27	69 ± 48	70 ± 172	136 ± 260	37 ± 24	63 ± 61
94ZW103	C	CCR5	8 ± 7	17 ± 10	5 ± 4	27 ± 32	83 ± 208	151 ± 277	4 ± 3	10 ± 6
UG270	D	CCR5	300 ± 461	508 ± 671	61 ± 32	182 ± 96	149 ± 91	430 ± 289	53 ± 28	107 ± 48
CM235	E	CCR5	39 ± 33	123 ± 99	9 ± 6	43 ± 33	17 ± 12	93 ± 39	11 ± 7	36 ± 22
BZ162	F	CCR5	10 ± 9	39 ± 32	5 ± 7	25 ± 25	67 ± 176	139 ± 273	4 ± 6	9 ± 11

[a] Pooled PBMCs from four human donors were used in the viral infectivity assay. Values are means and standard errors from the number of determinations indicated for each peptide ($n = x$).

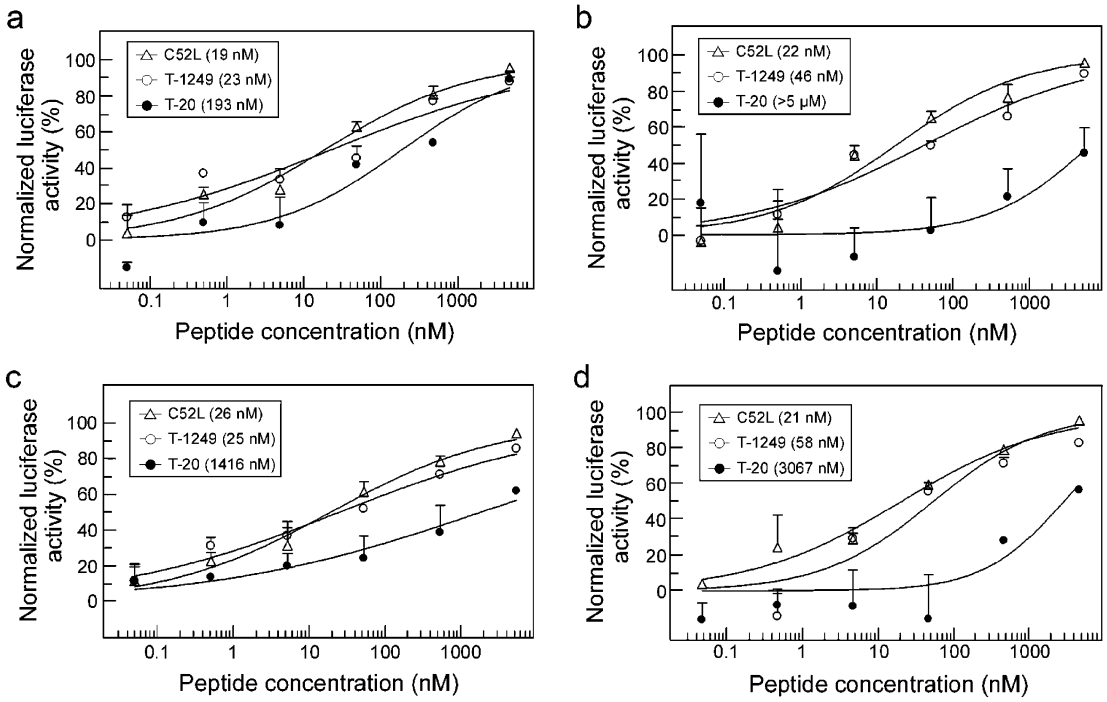

FIGURE 6: Inhibition of T-20-resistant pseudoviral infection by C52L. Recombinant HIV-1 viruses expressing firefly luciferase and incorporating the wild-type (a) or mutant GIA (b), GIM (c), and DIV (d) Env_{JFRL} glycoproteins were used to infect U87-$CD4^+$-$CCR5^+$ cells in the presence of C-peptides. Virus infection was measured after 72 h by determining luciferase expression in relative light units (RLU). The percentage of luciferase activity measured in the target cells relative to that observed in the absence of inhibitor is shown. The data represent the mean and standard error of duplicate points. The results shown are typical of those obtained in three experiments. The IC_{50} values obtained by curve fitting are given in parentheses in the inset.

viral population *in vitro* and the viral quasispecies of patients on T-20 therapy revealed the acquisition of resistant mutations in the highly conserved HR_N Gly-Ile-Val sequence motif (at positions 547 to 549) (*53*, *62*−*65*). As noted above, C52D and C52L include the critical sequence determinants of both T-20 and C34, suggesting that the recombinant peptides might be effective inhibitors of drug-resistant viruses. We therefore introduced three T-20-resistance mutations (Gly-Ile-*Ala*, Gly-Ile-*Met*, and *Asp*-Ile-Val) individually into the JFRL molecular clone and determined their impact on the antiviral activity of C52L in a single-cycle Env-mediated infection assay (Figure 6). As expected, C52L shows clear inhibitory activity against the $HIV\text{-}1_{JFRL}$, GIA, GIM, and DIV pseudovirions, with IC_{50} values of 19, 22, 26, and 21 nM, respectively. In parallel studies, the GIA, GIM, and DIV substitutions decrease T-20 sensitivity by >26-, 7-, and 16-fold, respectively. A positive control, the T-1249 peptide, exhibits similar effective inhibition of the wild-type and mutant viruses (the IC_{50} ranging from 23 to 58 nM), in accord with the previously reported activity of this synthetic 39-residue peptide (*56*). Taken together, these results demonstrate that C52L can provide the basis for the design and optimization of the next generation of HIV-1 fusion inhibitors.

DISCUSSION

In principle, formation of a stable postfusion six-helix bundle in gp41 is mechanistically and thermodynamically coupled to HIV-1 membrane fusion (*11*, *12*). Current thinking postulates that the receptor-induced activation of gp41 involves a regulated sequence of structural transitions with one or more on-pathway intermediate(s), although few details of these molecular events are understood. Consistent with this model for gp41 function, a large body of evidence indicates that the HR_N and HR_C regions, initially sequestered in the native Env glycoprotein spike, are sequentially released and refolded to drive membrane fusion (*17*, *22*−*25*). In this gp41 refolding process, a prehairpin intermediate containing

the N-peptide coiled-coil trimer is formed; this trimer is proposed to serve as a target for C-peptide inhibitors such as T-20 and C34 (*11*). These exogenous C-peptides bind in a dominant-negative manner to the gp41 N-peptide region and disrupt HIV-1 fusion by preventing subsequent folding into the six-helix bundle (*17*, *22*−*25*). Although T-20 and C34 are thought to have a similar mechanism of action, significant differences have been observed among their respective potencies in different HIV-1 isolates and in their sensitivities to resistant mutations (*53*−*55*).

In this study, we use a protein engineering method to present the entire C-peptide region (comprising the C34 and T-20 sequences) in a structured conformation toward the development of potent and broadly effective bacterially expressed inhibitory peptides. We have shown that the chimeric C52D and C52L molecules are folded into an α-helical structure at low temperatures and bind to the 5-helix protein with high affinity. Both C52D and C52L efficiently inhibit cell−cell fusion and potently block infection of human peripheral blood mononuclear cells by a diverse range of primary HIV-1 isolates *in vitro*, with IC_{50} values in the nanomolar range. In a previous study, C52L was shown to exhibit significant microbicidal activity in the macaque vaginal challenge model and to increase the capacities of the CCR5 ligand CMPD167 and the entry inhibitor BMS-378806 to protect rhesus macaques against infection by the CCR5 virus SHIV-162P3 (*9*).

The engineered C52L peptide has several attractive features that are relevant to possible applications to treat or prevent HIV-1 infection. First, the concentration of T-20 needed to inhibit drug-naive primary viruses can vary by at least two logs, and drug-resistant isolates have emerged both *in vitro* and *in vivo* (*9*, *62*−*65*). We find that C52L is a potent and broad inhibitor of viral infection and remains fully active against T-20-resistant HIV-1 strains. This property is consistent with the notion that the T-20 C-terminal tryptophan-rich region whose function is still unknown likely exerts antiviral activity independently from the proposed mechanism of inhibition of six-helix bundle formation (*52*, *54*, *55*). Thus, the C52L inhibitor has two different targets in gp41, and can help combat the global sequence diversity of HIV-1 and minimize the transmission of T-20-resistant viruses. This feature also makes C52L attractive as a probe to study the mechanism of action of T-20 and understand how its antiviral effect is mitigated by the evolution of resistant viruses *in vivo*. Second, the T-20 drug is manufactured by synthetic peptide chemistry (over 100 synthetic steps are involved), which is challenging and expensive when applied on a commercial scale.

We have shown that vaginally applied C52L, formulated in a simple gel, was able to protect rhesus macaques from vaginal challenge with a SHIV in a stringent model of HIV-1 sexual transmission (*9*). Moreover, C52L acts synergistically with the CCR5 ligand CMPD167 or the entry inhibitor BMS-378806 when inhibiting HIV-1 and SHIV replication *in vitro* (*9*). This renders it particularly suitable for use in a microbicide based on combinations of entry inhibitors (*8*, *9*). The bacterial expression of the C52L peptide could facilitate its production on a large scale at an economical cost, which is particularly important for microbicides intended for use in the developing world (*8*). Finally, for peptide-based vaginal microbicides, proteolytic activity at mucosal sites can be a major obstacle to potency and effective residence times. The enhanced helix stabilization of C52L may therefore be beneficial for increasing the extent and duration of its antiviral activity at the site of virus deposition by reducing its rate of degradation.

Interestingly, the epitopes of several broadly neutralizing human monoclonal antibodies directed against gp41 (*e.g.*, 2F5 and 4E10) are located immediately C terminal to the C-peptide region in the C52D and C52L constructs (*66*). All attempts to elicit anti-gp41 antibodies comparable to these elicited in infected humans by using unstructured C-peptide immunogens have thus far met with limited success. Clearly, there are critical and likely structural aspects of the 2F5 and 4E10 epitopes *in situ* on the trimeric Env complex that remain to be identified and exploited (*67*). Our finding that the C52D peptide self-associates into a labile helical trimer suggests that it may be possible to design and produce novel immunogens that stably present trimeric, α-helical conformation of the 2F5 and 4E10 epitopes in efforts to elicit broadly neutralizing antibodies to HIV-1.

ACKNOWLEDGMENT

We thank Per Johan Klasse for advice on antiviral data analysis, Brian Sullivan for technical assistance, and Neville Kallenbach for comments on the manuscript.

REFERENCES

1. Richman, D. D. (2001) HIV chemotherapy, *Nature 410*, 995−1001.
2. Pillay, D., Taylor, S., and Richman, D. D. (2000) Incidence and impact of resistance against approved antiretroviral drugs, *Rev. Med. Virol. 10*, 231−253.
3. Moore, J. P., and Stevenson, M. (2000) New targets for inhibitors of HIV-1 replication, *Nat. Rev. Mol. Cell Biol. 1*, 40−49.
4. Kuritzkes, D. R. (1996) Clinical significance of drug resistance in HIV-1 infection, *AIDS 10* (Suppl. 5), S27−31.
5. Coffin, J. M. (1995) HIV population dynamics in vivo: implications for genetic variation, pathogenesis, and therapy, *Science 267*, 483−489.
6. Mansky, L. M., Pearl, D. K., and Gajary, L. C. (2002) Combination of drugs and drug-resistant reverse transcriptase results in a multiplicative increase of human immunodeficiency virus type 1 mutant frequencies, *J. Virol. 76*, 9253−9259.
7. Matthews, T., Salgo, M., Greenberg, M., Chung, J., DeMasi, R., and Bolognesi, D. (2004) Enfuvirtide: the first therapy to inhibit the entry of HIV-1 into host CD4 lymphocytes, *Nat. Rev. Drug Discovery 3*, 215−225.
8. Klasse, P. J., Shattock, R. J., and Moore, J. P. (2006) Which topical microbicides for blocking HIV-1 transmission will work in the real world?, *PLoS Med. 3*.
9. Veazey, R. S., Klasse, P. J., Schader, S. M., Hu, Q., Ketas, T. J., Lu, M., Marx, P. A., Dufour, J., Colonno, R. J., Shattock, R. J., Springer, M. S., and Moore, J. P. (2005) Protection of macaques from vaginal SHIV challenge by vaginally delivered inhibitors of virus-cell fusion, *Nature 438*, 99−102.
10. Hunter, E., and Swanstrom, R. (1990) Retrovirus envelope glycoproteins, *Curr. Top. Microbiol. Immunol. 157*, 187−253.
11. Eckert, D. M., and Kim, P. S. (2001) Mechanisms of viral membrane fusion and its inhibition, *Annu. Rev. Biochem. 70*, 777−810.
12. Harrison, S. C. (2005) Mechanism of membrane fusion by viral envelope proteins, *Adv. Virus Res. 64*, 231−261.
13. Moore, J. P., and Doms, R. W. (2003) The entry of entry inhibitors: a fusion of science and medicine, *Proc. Natl. Acad. Sci. U.S.A. 100*, 10598−10602.
14. Chan, D. C., Fass, D., Berger, J. M., and Kim, P. S. (1997) Core structure of gp41 from the HIV envelope glycoprotein, *Cell 89*, 263−273.

15. Tan, K., Liu, J., Wang, J., Shen, S., and Lu, M. (1997) Atomic structure of a thermostable subdomain of HIV-1 gp41, *Proc. Natl. Acad. Sci. U.S.A. 94*, 12303−12308.
16. Weissenhorn, W., Dessen, A., Harrison, S. C., Skehel, J. J., and Wiley, D. C. (1997) Atomic structure of the ectodomain from HIV-1 gp41, *Nature 387*, 426−430.
17. Lu, M., Blacklow, S. C., and Kim, P. S. (1995) A trimeric structural domain of the HIV-1 transmembrane glycoprotein, *Nat. Struct. Biol. 2*, 1075−1082.
18. Skehel, J. J., and Wiley, D. C. (2000) Receptor binding and membrane fusion in virus entry: the influenza hemagglutinin, *Annu. Rev. Biochem. 69*, 531−569.
19. Jiang, S., Lin, K., Strick, N., and Neurath, A. R. (1993) HIV-1 inhibition by a peptide, *Nature 365*, 113.
20. Wild, C. T., Shugars, D. C., Greenwell, T. K., McDanal, C. B., and Matthews, T. J. (1994) Peptides corresponding to a predictive alpha-helical domain of human immunodeficiency virus type 1 gp41 are potent inhibitors of virus infection, *Proc. Natl. Acad. Sci. U.S.A. 91*, 9770−9774.
21. Kilby, J. M., Hopkins, S., Venetta, T. M., DiMassimo, B., Cloud, G. A., Lee, J. Y., Alldredge, L., Hunter, E., Lambert, D., Bolognesi, D., Matthews, T., Johnson, M. R., Nowak, M. A., Shaw, G. M., and Saag, M. S. (1998) Potent suppression of HIV-1 replication in humans by T-20, a peptide inhibitor of gp41-mediated virus entry, *Nat. Med. 4*, 1302−1307.
22. Chen, C. H., Matthews, T. J., McDanal, C. B., Bolognesi, D. P., and Greenberg, M. L. (1995) A molecular clasp in the human immunodeficiency virus (HIV) type 1 TM protein determines the anti-HIV activity of gp41 derivatives: implication for viral fusion, *J. Virol. 69*, 3771−3777.
23. Furuta, R. A., Wild, C. T., Weng, Y., and Weiss, C. D. (1998) Capture of an early fusion-active conformation of HIV-1 gp41, *Nat. Struct. Biol. 5*, 276−279.
24. Wild, C., Greenwell, T., Shugars, D., Rimsky-Clarke, L., and Matthews, T. (1995) The inhibitory activity of an HIV type 1 peptide correlates with its ability to interact with a leucine zipper structure, *AIDS Res. Hum. Retroviruses 11*, 323−325.
25. Chan, D. C., and Kim, P. S. (1998) HIV entry and its inhibition, *Cell 93*, 681−684.
26. Lu, M., and Kim, P. S. (1997) A trimeric structural subdomain of the HIV-1 transmembrane glycoprotein, *J. Biomol. Struct. Dyn. 15*, 465−471.
27. Judice, J. K., Tom, J. Y., Huang, W., Wrin, T., Vennari, J., Petropoulos, C. J., and McDowell, R. S. (1997) Inhibition of HIV type 1 infectivity by constrained alpha-helical peptides: implications for the viral fusion mechanism, *Proc. Natl. Acad. Sci. U.S.A. 94*, 13426−13430.
28. Shu, W., Liu, J., Ji, H., Radigen, L., Jiang, S., and Lu, M. (2000) Helical interactions in the HIV-1 gp41 core reveal structural basis for the inhibitory activity of gp41 peptides, *Biochemistry 39*, 1634−1642.
29. Sia, S. K., Carr, P. A., Cochran, A. G., Malashkevich, V. N., and Kim, P. S. (2002) Short constrained peptides that inhibit HIV-1 entry, *Proc. Natl. Acad. Sci. U.S.A. 99*, 14664−14669.
30. Sia, S. K., and Kim, P. S. (2003) Protein grafting of an HIV-1-inhibiting epitope, *Proc. Natl. Acad. Sci. U.S.A. 100*, 9756−9761.
31. Jin, B. S., Ryu, J. R., Ahn, K., and Yu, Y. G. (2000) Design of a peptide inhibitor that blocks the cell fusion mediated by glycoprotein 41 of human immunodeficiency virus type 1, *AIDS Res. Hum. Retroviruses 16*, 1797−1804.
32. Doering, D. S., and Matsudaira, P. (1996) Cysteine scanning mutagenesis at 40 of 76 positions in villin headpiece maps the F-actin binding site and structural features of the domain, *Biochemistry 35*, 12677−12685.
33. Kunkel, T. A., Roberts, J. D., and Zakour, R. A. (1987) Rapid and efficient site-specific mutagenesis without phenotypic selection, *Methods Enzymol. 154*, 367−382.
34. Abrahamyan, L. G., Mkrtchyan, S. R., Binley, J., Lu, M., Melikyan, G. B., and Cohen, F. S. (2005) The cytoplasmic tail slows the folding of human immunodeficiency virus type 1 Env from a late prebundle configuration into the six-helix bundle, *J. Virol. 79*, 106−115.
35. Edelhoch, H. (1967) Spectroscopic determination of tryptophan and tyrosine in proteins, *Biochemistry 6*, 1948−1954.
36. Chen, Y. H., Yang, J. T., and Chau, K. H. (1974) Determination of the helix and beta form of proteins in aqueous solution by circular dichroism, *Biochemistry 13*, 3350−3359.
37. Johnson, M. L., Correia, J. J., Yphantis, D. A., and Halvorson, H. R. (1981) Analysis of data from the analytical ultracentrifuge by nonlinear least-squares techniques, *Biophys. J. 36*, 575−588.
38. Laue, T. M., Shah, B. D., Ridgeway, T. M., and Pelletier, S. L. (1992) in *Analytical Ultracentrifugation in Biochemistry and Polymer Science* (Harding, S. E., Rowe, A. J., and Horton, J. C., Eds.) pp 90−125, Royal Society of Chemistry, Cambridge.
39. Kozarsky, K., Penman, M., Basiripour, L., Haseltine, W., Sodroski, J., and Krieger, M. (1989) Glycosylation and processing of the human immunodeficiency virus type 1 envelope protein, *J. Acquired Immune Defic. Syndr. 2*, 163−169.
40. Trkola, A., Matthews, J., Gordon, C., Ketas, T., and Moore, J. P. (1999) A cell line-based neutralization assay for primary human immunodeficiency virus type 1 isolates that use either the CCR5 or the CXCR4 coreceptor, *J. Virol. 73*, 8966−8974.
41. Ketas, T. J., Klasse, P. J., Spenlehauer, C., Nesin, M., Frank, I., Pope, M., Strizki, J. M., Reyes, G. R., Baroudy, B. M., and Moore, J. P. (2003) Entry inhibitors SCH-C, RANTES, and T-20 block HIV type 1 replication in multiple cell types, *AIDS Res. Hum. Retroviruses 19*, 177−186.
42. Trkola, A., Paxton, W. A., Monard, S. P., Hoxie, J. A., Siani, M. A., Thompson, D. A., Wu, L., Mackay, C. R., Horuk, R., and Moore, J. P. (1998) Genetic subtype-independent inhibition of human immunodeficiency virus type 1 replication by CC and CXC chemokines, *J. Virol. 72*, 396−404.
43. Mosmann, T. (1983) Rapid colorimetric assay for cellular growth and survival: application to proliferation and cytotoxicity assays, *J. Immunol. Methods 65*, 55−63.
44. Beddows, S., Schulke, N., Kirschner, M., Barnes, K., Franti, M., Michael, E., Ketas, T., Sanders, R. W., Maddon, P. J., Olson, W. C., and Moore, J. P. (2005) Evaluating the immunogenicity of a disulfide-stabilized, cleaved, trimeric form of the envelope glycoprotein complex of human immunodeficiency virus type 1, *J. Virol. 79*, 8812−8827.
45. Herrera, C., Spenlehauer, C., Fung, M. S., Burton, D. R., Beddows, S., and Moore, J. P. (2003) Nonneutralizing antibodies to the CD4-binding site on the gp120 subunit of human immunodeficiency virus type 1 do not interfere with the activity of a neutralizing antibody against the same site, *J. Virol. 77*, 1084−1091.
46. Gordon, C. J., Muesing, M. A., Proudfoot, A. E., Power, C. A., Moore, J. P., and Trkola, A. (1999) Enhancement of human immunodeficiency virus type 1 infection by the CC-chemokine RANTES is independent of the mechanism of virus-cell fusion, *J. Virol. 73*, 684−694.
47. Wild, C., Oas, T., McDanal, C., Bolognesi, D., and Matthews, T. (1992) A synthetic peptide inhibitor of human immunodeficiency virus replication: correlation between solution structure and viral inhibition, *Proc. Natl. Acad. Sci. U.S.A. 89*, 10537−10541.
48. Chan, D. C., Chutkowski, C. T., and Kim, P. S. (1998) Evidence that a prominent cavity in the coiled coil of HIV type 1 gp41 is an attractive drug target, *Proc. Natl. Acad. Sci. U.S.A. 95*, 15613−15617.
49. Eckert, D. M., Malashkevich, V. N., Hong, L. H., Carr, P. A., and Kim, P. S. (1999) Inhibiting HIV-1 entry: discovery of D-peptide inhibitors that target the gp41 coiled-coil pocket, *Cell 99*, 103−115.
50. Zhou, G., Ferrer, M., Chopra, R., Kapoor, T. M., Strassmaier, T., Weissenhorn, W., Skehel, J. J., Oprian, D., Schreiber, S. L., Harrison, S. C., and Wiley, D. C. (2000) The structure of an HIV-1 specific cell entry inhibitor in complex with the HIV-1 gp41 trimeric core, *Bioorg. Med. Chem. 8*, 2219−2227.
51. Ferrer, M., Kapoor, T. M., Strassmaier, T., Weissenhorn, W., Skehel, J. J., Oprian, D., Schreiber, S. L., Wiley, D. C., and Harrison, S. C. (1999) Selection of gp41-mediated HIV-1 cell entry inhibitors from biased combinatorial libraries of non-natural binding elements, *Nat. Struct. Biol. 6*, 953−960.
52. Liu, S., Lu, H., Niu, J., Xu, Y., Wu, S., and Jiang, S. (2005) Different from the HIV fusion inhibitor C34, the anti-HIV drug Fuzeon (T-20) inhibits HIV-1 entry by targeting multiple sites in gp41 and gp120, *J. Biol. Chem. 280*, 11259−11273.
53. Rimsky, L. T., Shugars, D. C., and Matthews, T. J. (1998) Determinants of human immunodeficiency virus type 1 resistance to gp41-derived inhibitory peptides, *J. Virol. 72*, 986−993.
54. Reeves, J. D., Miamidian, J. L., Biscone, M. J., Lee, F. H., Ahmad, N., Pierson, T. C., and Doms, R. W. (2004) Impact of mutations in the coreceptor binding site on human immunodeficiency virus type 1 fusion, infection, and entry inhibitor sensitivity, *J. Virol. 78*, 5476−5485.

55. Kliger, Y., Gallo, S. A., Peisajovich, S. G., Munoz-Barroso, I., Avkin, S., Blumenthal, R., and Shai, Y. (2001) Mode of action of an antiviral peptide from HIV-1. Inhibition at a post-lipid mixing stage, *J. Biol. Chem. 276*, 1391−1397.
56. Eron, J. J., Gulick, R. M., Bartlett, J. A., Merigan, T., Arduino, R., Kilby, J. M., Yangco, B., Diers, A., Drobnes, C., DeMasi, R., Greenberg, M., Melby, T., Raskino, C., Rusnak, P., Zhang, Y., Spence, R., and Miralles, G. D. (2004) Short-term safety and antiretroviral activity of T-1249, a second-generation fusion inhibitor of HIV, *J. Infect. Dis. 189*, 1075−1083.
57. Shu, W., Ji, H., and Lu, M. (1999) Trimerization specificity in HIV-1 gp41: analysis with a GCN4 leucine zipper model, *Biochemistry 38*, 5378−5385.
58. Cao, W., Bracken, C., Kallenbach, N. R., and Lu, M. (2004) Helix formation and the unfolded state of a 52-residue helical protein, *Protein Sci. 13*, 177−189.
59. Harbury, P. B., Kim, P. S., and Alber, T. (1994) Crystal structure of an isoleucine-zipper trimer, *Nature 371*, 80−83.
60. Root, M. J., Kay, M. S., and Kim, P. S. (2001) Protein design of an HIV-1 entry inhibitor, *Science 291*, 884−888.
61. Ketas, T., Schader, S. M., Zurita, J., Teo, E., Polonis, V., Lu, M., Klasse, P. J., and Moore, J. P. (2007) Entry inhibitor-based microbicides are active in vitro against HIV-1 isolates from multiple genetic subtypes, *Virology*, in press.
62. Poveda, E., Rodes, B., Toro, C., Martin-Carbonero, L., Gonzalez-Lahoz, J., and Soriano, V. (2002) Evolution of the gp41 env region in HIV-infected patients receiving T-20, a fusion inhibitor, *AIDS 16*, 1959−1961.
63. Kilby, J. M., Lalezari, J. P., Eron, J. J., Carlson, M., Cohen, C., Arduino, R. C., Goodgame, J. C., Gallant, J. E., Volberding, P., Murphy, R. L., Valentine, F., Saag, M. S., Nelson, E. L., Sista, P. R., and Dusek, A. (2002) The safety, plasma pharmacokinetics, and antiviral activity of subcutaneous enfuvirtide (T-20), a peptide inhibitor of gp41-mediated virus fusion, in HIV-infected adults, *AIDS Res. Hum. Retroviruses 18*, 685−693.
64. Wei, X., Decker, J. M., Liu, H., Zhang, Z., Arani, R. B., Kilby, J. M., Saag, M. S., Wu, X., Shaw, G. M., and Kappes, J. C. (2002) Emergence of resistant human immunodeficiency virus type 1 in patients receiving fusion inhibitor (T-20) monotherapy, *Antimicrob. Agents Chemother. 46*, 1896−1905.
65. Baldwin, C. E., Sanders, R. W., Deng, Y., Jurriaans, S., Lange, J. M., Lu, M., and Berkhout, B. (2004) Emergence of a drug-dependent human immunodeficiency virus type 1 variant during therapy with the T20 fusion inhibitor, *J. Virol. 78*, 12428−12437.
66. Zwick, M. B., Jensen, R., Church, S., Wang, M., Stiegler, G., Kunert, R., Katinger, H., and Burton, D. R. (2005) Anti-human immunodeficiency virus type 1 (HIV-1) antibodies 2F5 and 4E10 require surprisingly few crucial residues in the membrane-proximal external region of glycoprotein gp41 to neutralize HIV-1, *J. Virol. 79*, 1252−1261.
67. Burton, D. R., Desrosiers, R. C., Doms, R. W., Koff, W. C., Kwong, P. D., Moore, J. P., Nabel, G. J., Sodroski, J., Wilson, I. A., and Wyatt, R. T. (2004) HIV vaccine design and the neutralizing antibody problem, *Nat. Immunol. 5*, 233−236.
68. Kleid, D. G., Yansura, D., Small, B., Dowbenko, D., Moore, D. M., Grubman, M. J., McKercher, P. D., Morgan, D. O., Robertson, B. H., and Bachrach, H. L. (1981) Cloned viral protein vaccine for foot-and-mouth disease: responses in cattle and swine, *Science 214*, 1125−1129.

BI7001289